

Dynamic Modelling of Fuel Cell Systems for Electric Propulsion

Nastaran Shakeri
Department of Marine Technology
Norwegian University of Science and Technology
Trondheim, Norway
nastaran.shakeri@ntnu.no

Mehdi Zadeh
Department of Marine Technology
Norwegian University of Science and Technology
Trondheim, Norway
mehdi.zadeh@ntnu.no

Abstract—In this paper, a dynamic model is developed for hybrid electric powertrains with fuel cell and batteries. The hybrid powertrain is considered mainly for marine propulsion with dynamic load, although the study can be generalized to other types of transportation. The dynamic model is established based on equivalent circuit models of fuel cell, battery, and converter interfaces. The effect of the fuel flow rate is also included in the system model incorporating with the equivalent circuit of the fuel cell. The battery is used as energy storage and mainly for the peak shaving under transient loads and peak loads. The simulation results are presented such as load sharing between the fuel cell and battery under various load conditions.

Keywords—Hybrid electric propulsion, fuel cells, batteries, electric circuit modeling, hydrogen fuel, marine power systems.

I. INTRODUCTION

Emission production from marine propulsion is a major issue to overcome both for international shipping and short-route marine transport [1]. Hence, ship owners need to adopt solutions for decarbonization within existing and emerging environmental regulations. Among several ways to reduce emission from shipping, alternative fuels with low carbon intensity – usually in the form of gaseous or other low flash point fuels – are attractive [2]. Hydrogen (H_2), with its apparently carbon-free characteristics, is a candidate alternative fuel. In comparison with existing fuels, H_2 has a high specific energy (about 142 MJ/kg), but in the form of gas has relatively low energy density at standard temperature and pressure (about 0.01079 MJ/L) [3]. Higher specific energy means longer operation range with less refueling frequency and lower ship weight, although low energy density brings the issue of fuel storage and transport. Hence, liquid hydrogen (LH_2) and other forms of the fuel, such as methane and ammonia, are rather attractive for long-distance shipping.

The alternative fuels can be used either in internal combustion engines (ICE) or fuel cells (FC). It is difficult to remain the stable fuel efficiency with ICE, mainly due to the high self-ignition temperature of H_2 (858 K) which necessitates temperature control of the inlet air. Moreover, for higher temperatures, the auto ignition delay increases rapidly, hence, H_2 injection/fuel flow rate must be controlled to obtain the required dynamic response. Alternatively, FCs convert the chemical energy of the reactants to electrical energy without any combustion process, which results in lower energy loss and higher total efficiency. FCs consume less liquid hydrogen compared to ICEs, requiring less space onboard for the same route [4]. FCs are also scalable, means that individual FCs can be joined with one another to form stacks and build larger electric propulsions, such as multi-megawatt installations. FC stacks can be connected to shape the FC modules based on the required voltage and current, in series, parallel or combination

of series and parallel. The scalability of the FC systems brings less dependability and higher reliability compared to larger marine engines.

Different types of FC systems are available which can be categorized on operating temperature. A common classification is high temperature FCs (HTFCs) such as Solid Oxide FC (SOFC), with operating temperature up to 1100°C, and low temperature FCs (LTFCs) like polymer electrolyte membrane FC (PEMFC), with operating temperature from 60°C to 120°C. The low tolerance of LTFCs to the H_2 impurity reduces its electrical efficiency based on LHV with air as oxidant comparing to HTFCs. However, HTFCs require fuel processing equipment to process H_2 of lower quality which can increase the total system size, cost, weight and load-following capabilities [5]. Increased size/dimensioning may result in lower power density (W/kg) compared to the PEMFC which is simpler to control. Different types of FCs also have different causes of failure. The critical issues in FCs failure are water management and heat exchange system. HTFCs can fail because of high operating temperatures, while in LTFCs designing water management system is of high importance [6]. Both PEMFC and SOFC are attractive for marine propulsion, although, low temperature PEMs are very common in the existing market mainly due to the rather mature technology and higher safety margin. PEMFCs are available for onboard applications from small and medium size to MW scale.

FCs have good partly load characteristics, because increasing in mechanical losses has effect only on parasitic load of its auxiliary components [3]. However, the behaviour of a PEMFC is characterized by its slow dynamic response, unregulated terminal voltage as a function of output current and reactants flow rate, and unidirectional power flow. Yet, these drawbacks can be compensated in a hybrid power system thanks to the energy storage systems (ESS) [7]. Electric and hybrid powertrains are increasingly under research and development for both short-sea and long distance shipping. Such hybrid power systems are normally established based on clean power sources, e.g., fuel cells, and energy storages, such as batteries and supercapacitors, which are connected often through a dc microgrid or dc switchboard (see Fig. 1). Then the FCs can operate as main source of power and the ESS can be dimensioned to provide enhanced dynamic support when it comes to fast load transients or overloads. The ratio of FC dimensioning to the ESS depends on the vessel operational profile such as the load demand.

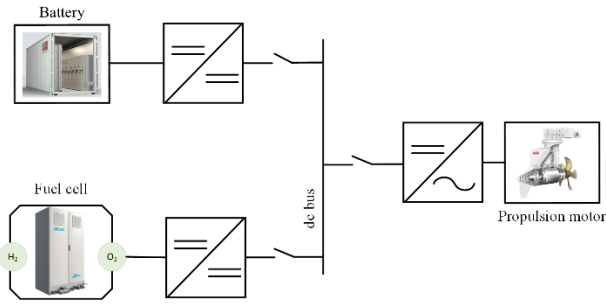


Fig. 1. FC powered marine vessel system with dc distribution.

Yet, the dynamic behavior of such emerging systems is less investigated, while the system design in different phases require understanding of the dynamic modes such as interactions between power sources, power electronics, and control layers. The FC models which are used in power system study in the literature can be found in three classified groups including: analytical models based on thermodynamics, frequency-domain identification by impedance spectroscopy model, and empirical models. The analytical models need deep knowledge of the FC internal operation and thermodynamic reactions [8]. The second category obtains a frequency domain of electrochemical devices by specific experimental investigations [9]. The empirical models, model the behavior of FC in diverse methods from look up table to complex sets of equations. The empirical voltage model is based on three voltage drops in FC polarization curve which does not require a deep knowledge of the FC internal operation [10]. A typical polarization curve of FC includes three main areas: activation region, ohmic region, and concentration region which result in 3 voltage drops [11]. Authors in [12] used the empirical voltage model to control the dc bus voltage in hybrid FC and battery power systems in marine vessels.

Equivalent electrical circuit model can be used to show the dynamic responses of FC to load changes, and makes the evaluation of integration of the component to the rest of hybrid power system easier. It also can be used to build up series/parallel combination of FC stacks based on the operation design. In [13] a FC equivalent circuit model based on voltage overshoot transient response is introduced, where variable parameter is used for representing FC time constant. However, the physical interpretation of FC model used for system-level analysis should be straightforward to accurately describe the FC voltage behavior during high-dynamic current profiles.

The power electronics interfaces such as dc-dc converters play an essential role in the energy management of hybrid power systems. This allows voltage conversion as well as full control of output current and dc bus voltage. The local controller for dc-dc converter in onboard microgrid can be designed in two ways: grid forming and grid following. In grid forming mode, dc-dc converter operates as a voltage source and the converter controller is designed in a way that be responsible for maintaining dc bus voltage by controlling the power supplied to the grid. The regulated dc voltage level is required to keep the system stability and persistent load supply [14]. Controlling dc bus voltage level also results in reducing losses in power electronics and magnetic devices. On contrary, when there is no voltage setpoint and the converter controller receives only a power/current setpoint, the converter operates in the so-called grid following mode, and

is seen from the output as a current source. In this case, the FC converter is assumed to operate in the grid-forming mode, while the battery converter acts as grid-following converter. For system-level analysis, averaged model of converters is an acceptable approach, where the exact switching behavior is replaced with the dynamic averaged switch modeling resulting in higher computational efficiency [14].

In this paper, an equivalent circuit model for FC-based electric propulsion system is developed comprising the main elements of the power system and the main control functions. The circuit model is developed as an active equivalent circuit which is dynamically adopting to the control dynamics. The presented model has passive and active components. The passive components are derived from the FC (static and dynamic) behavior as well as the system design outfit. For the static parameters, the manufacturer data is used. The active elements are derived from the control system integrated into the averaged model of dc-dc converters. The dynamic effect of fuel flow rate is also considered in the FC modeling as an active element. At the end the model is verified under various load-sharing scenarios and time-domain simulation results are presented. The simulation results prove the effectiveness of the presented model to capture main system dynamics under steady-state as well as transient conditions.

II. HYBRID POWER SYSTEM MODEL AND CONTROLLER

In this section, the model of hybrid power system and the related controller are explained. To meet variable power requirements of vessels, FCs can integrate in series, parallel or combination of series and parallel. The chosen combination includes The FC is 50 kW, 625Vdc PEMFC consists of 14, 6kW, 45Vdc PEMFCs connected in series and are incorporated to the dc bus with the common dc-dc converter in grid forming mode. In this design all modules are controlled together. The battery is 30 kWh which is connected to the dc bus with the bidirectional dc-dc converter in grid following mode. Propulsion motors and other onboard hotel loads are connected to the dc bus with dedicated load converters. The propulsion system in this work is modeled as a constant power loads (CPL), where load power is tightly controlled by the load converters for propulsion loads [15].

The averaged switch model for dc-dc converters showed in Fig. 2 can be used as unified model for buck and boost mode [13]. The operation of the boost mode at duty cycle of “d” ($=1-d'$) corresponds to the operation of buck mode with only the opposite reference current flow direction (in the buck mode charging current is set to be positive, and in boost mode discharging current is negative). The control of the dc-dc converters is mostly done by proportional-integral (PI) controllers. In this work FC converter is in voltage mode control to stabilize the dc bus voltage (grid forming) and the battery converter is in current mode control (grid following) to meet power load variations. The PI controllers are also shown in Fig. 3. The FC converter controller has both inner current loop ($PI_i(s)$) and outer loop PI controller ($PI_v(s)$), with gains (K_p , and K_i) which are tuned based on the ordinary differential equations (ODEs) calculated based on the Thevenin model of FC and its dc-dc converter.

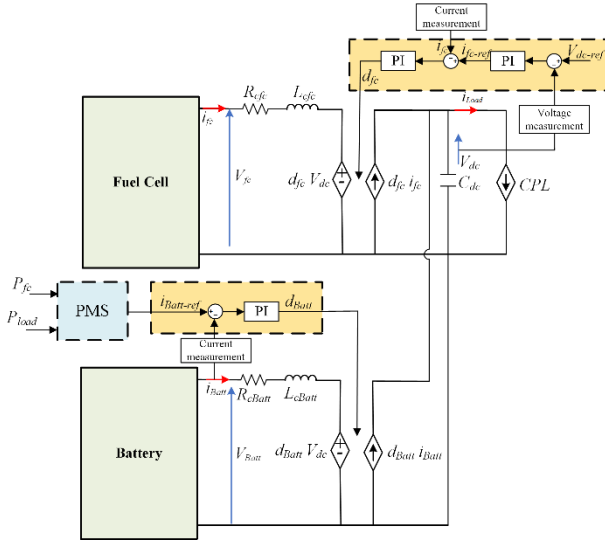


Fig. 2. Single line diagram (SLD) of electric propulsion system.

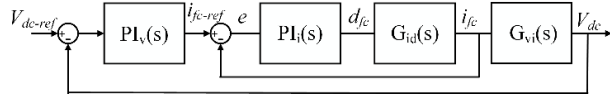


Fig. 3. Control block diagram for FC converter in grid forming mode

For inner loop current control after calculating the transfer functions in s-domain for $G_{id}(s)$ as (1), the $PI_i(s)$ gains will be obtained to calculate the duty cycle d_{fc} based on the FC current reference i_{fc-ref} generated by the outer voltage loop control to control the dc bus voltage V_{dc} as a output of outer transfer function $G_{vi}(s)$ in (2) where in the control input is the output of inner closed loop feedback control.

$$G_{id}(s) = \frac{i_{fc}(s)}{d_{fc}(s)} \quad (1)$$

$$G_{vi}(s) = \frac{V_{dc}(s)}{i_{fc}(s)} \quad (2)$$

For the battery dc-dc converter which is in current mode control the procedure to generate d_{Batt} is the same with the difference that there is only current measurement for battery side controller design with the inner loop, where the battery current reference $i_{Batt-ref} = P_{ref-Batt}/V_{Batt}$ is generated from the power management system (PMS) as (3):

$$P_{ref-Batt} = P_{load} - P_{fc} \quad (3)$$

Where P_{fc} is the power generated by FC and P_{load} is the shipboard power load. So, the peak shaving battery will meet the load variation demand while its dc-dc controller follows the required power calculated from PMS. Based on the $i_{Batt-ref}$ flow direction the battery is in charge or discharge mode [16]. The PI controller gains (K_p , and K_i) are obtained based on the ordinary differential equations (ODEs) calculated based on the Thevenin model of battery and its dc converter.

III. DEVELOPMENT OF ACTIVE CIRCUIT MODELS

The equivalent circuit model of FC is developed in the following, which is shown in Fig.4, where V_{oc} is the open circuit voltage, the variable resistor $R_v(i_{fc})$ model the static voltage drops of fuel cell including the ohmic loss and

activation voltage drop. The capacitor C_{fc} , and R_{fc} model the dynamic behavior of FC.

In this work the concentration losses is ignored and is not modeled because operation of FC in this region has significant impact on FC voltage only at high loads (above the nominal power of an FC) [12]. It is also assumed that the stack is made of identical cells.

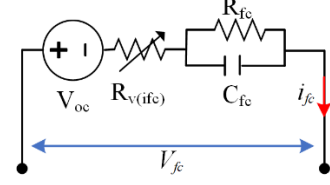


Fig. 4. Electrical equivalent circuit of FC model proposed.

A. Static model of FC

The first static parameter which can be measured based on polarization curve is V_{oc} . Fig. 3 shows the polarization curve of a 6kW, 45 Vdc FC. In this study, the MATLAB/Simulink FC model is used for modeling.

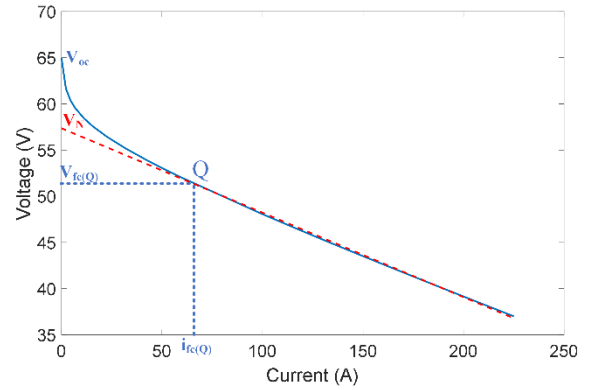


Fig. 5. Polarization curve of FC under study.

The resistor $R_v(i_{fc})$ is calculated by the ohmic drop between V_{oc} and FC output voltage V_{fc} , which has two parts: constant and variable based on the current. These parameters can be obtained from curve fitting of FC steady state performance. The constant value R_s is calculated by the linearized ohmic drop in ohmic region which is following the ohm law and is equal to (4), and the variable value is models as a resistor which represents the voltage drop below the operating point (Q) as (5).

$$R_s = (V_N - V_{fc(Q)})/i_{fc(Q)} \quad (4)$$

$$R_v = \frac{V_{oc} - (R_s \times i_{fc}) - V_{fc}}{i_{fc}} \quad (5)$$

After the operating point Q in Fig.5, the resistor is almost constant and in shipboard dc power system the centralized controller is designed in a way that FC operates in a way to supply partial load, and to avoid variable passive components in the modeling, the estimated constant value is considered for $R_v(i_{fc})$.

B. Dynamic model with averaged model of converters

Once the static equivalent circuit model of FC is identified as passive components, the dynamic parameters also can be obtained by applying the load current step and analyzing the voltage drops across the fuel cell voltage terminal by comparing the identified model and measured data. When a load current step applies, the FC voltage terminal changes instantaneously. This voltage change is due to both the static and dynamic parameters. The amount of R_{fc} is calculated by dividing the voltage drop $\Delta V_{transient}$ for each load current step Δi_{fc} , as (6):

$$R_{fc} = \frac{\Delta V_{transient}}{\Delta i_{fc}} \quad (6)$$

The voltage across the capacitor, C_{fc} is calculated by (7) which is a first order transfer function.

$$V_{C_{fc}} = \left(i_{fc} - C_{fc} \frac{dV_{C_{fc}}}{dt} \right) R_{fc} \quad (7)$$

The dynamic FC time constant τ_{fc} comprises of dynamic resistor R_{fc} , and dynamic capacitor C_{fc} . After calculating R_{fc} , the C_{fc} can be defined based on the dynamic time constant. In the model, C_{fc} is the equivalent capacitor due to the double-layer charging effect.

One of the advantages of the equivalent circuit modeling is that it makes the evaluation of integration of the component to the rest of shipboard power system more straightforward. Based on Fig. 6 the Thevenin model of FC and its dc-dc converter can be written as:

$$\frac{di_{fc}}{dt} = \frac{1}{L_{cfc}} (V_{oc-fc} - V_{C_{fc}} - R_{cfc} i_{fc} - d_{fc} V_{dc}) \quad (8)$$

$$\frac{dV_{dc}}{dt} = \frac{1}{C_{dc}} (-i_{load} + d_{fc} i_{fc}) \quad (9)$$

$$\frac{dV_{C_{fc}}}{dt} = \frac{1}{C_{fc}} \left(i_{fc} - \frac{V_{C_{fc}}}{R_{fc}} \right) \quad (10)$$

Where R_{cfc} and L_{cfc} are dc-dc converter parameters. d_{fc} is dc-dc converter duty cycle. So, the FC and its dc-dc converter can be seen as a one component from dc link, which based on the design in this work acts as a voltage source to form the onboard microgrid and keep the dc bus voltage constant.

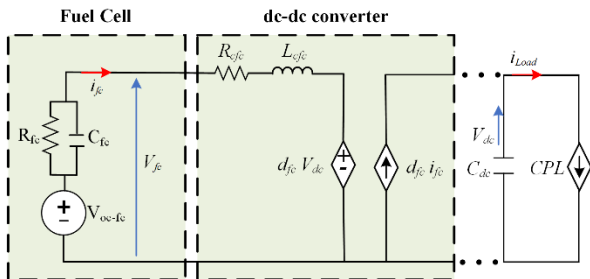


Fig. 6. Electrical equivalent circuit of FC and dc-dc converter.

In this work for the battery model, first order Thevenin battery model is used to present dynamic behavior of the battery. The model consists of open circuit voltage $V_{oc-Batt}$, and RC parallel circuit with resistor R_{Batt} , and capacitor

C_{Batt} , which is shown in Fig. 7 with its dc-dc converter. Battery like FC is dc power source with characteristics of variable terminal voltage which is a function of output current. Thevenin model of battery and its dc-dc converter can be written as:

$$\frac{di_{Batt}}{dt} = \frac{1}{L_{cBatt}} (V_{oc-Batt} - V_{C_{Batt}} - R_{cBatt} i_{Batt} - d_{Batt} V_{dc}) \quad (11)$$

$$\frac{dV_{dc}}{dt} = \frac{1}{C_{dc}} (-i_{load} + d_{Batt} i_{Batt}) \quad (12)$$

$$\frac{dV_{C_{Batt}}}{dt} = \frac{1}{C_{Batt}} \left(i_{Batt} - \frac{V_{C_{Batt}}}{R_{Batt}} \right) \quad (13)$$

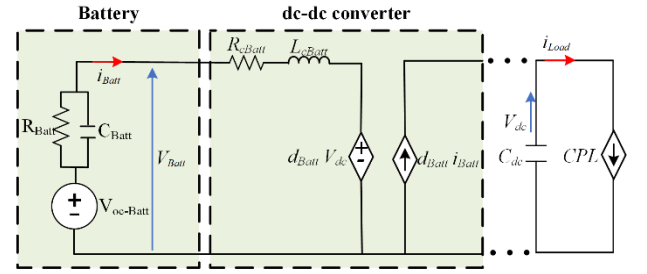


Fig. 7. Electrical equivalent circuit of Battery and dc-dc converter.

Hence based on the battery current flow reference direction, the battery's mode will change as (14):

$$\begin{cases} \text{Discharge mode: } V_{oc-Batt} > d_{Batt} V_{dc} \\ \text{Disconnect: } V_{oc-Batt} = d_{Batt} V_{dc} \\ \text{Charge mode: } V_{oc-Batt} < d_{Batt} V_{dc} \end{cases} \quad (14)$$

Where d_{Batt} is duty cycle of the averaged model dc-dc converter connected to the battery, $V_{oc-Batt}$ is the open circuit voltage of battery. The battery dc-dc converter is in grid following mode so the battery and its converter act as a current source to compensate for slow dynamic of FC.

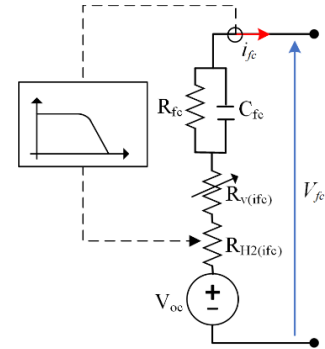


Fig. 8. Electrical equivalent circuit of FC model proposed.

C. Effect of hydrogen flow

The effect of fuel flow rate F_f also considered in this system-level modeling which is modeled as a low pass filter as $F_f(s) = \frac{k_f}{1+\tau s}$. The delay τ is due to the dynamics of the governor system. The gain k_f demonstrates that fuel flow rate is a proportional function of FC output current. In this work the effect of fuel flow rate is modeled as a variable resistance $R_{H_2}(i_{fc})$ which is shown in Fig. 8 by considering that other FC parameters are remaining approximately constant, including temperature, pressure, fuel and oxidant

composition, and etc. Increasing load current requires more hydrogen to be consumed in the anode channel. $R_{H_2}(i_{fc})$ is calculated based on the transient changes in FC terminal voltage by applying current load step change which is shown in the next part.

IV. RESULTS AND DISCUSSIONS

In this section, the simulation models are used for the dynamic analysis. To validate the FC electrical equivalent circuit model and averaged model of dc-dc converters based on their local controllers, two load sharing strategies are considered for the central load sharing. First the FC is designed for average power and in the second scenario FC is used for range extender. In both load sharing, the shipboard load profile is considered the same, with step changes in CPL to check the proposed control method. Among several functions of batteries in shipboard dc power system, in this work battery is in peak shaving mode where battery either charge or discharge depending on the load variations, while ensures that the FC slow power slope is compensated.

Without considering any losses in connecting FCs in series to scale up the FC output power, 50 kW, 625Vdc PEMFC consists of 14, 6kW, 45Vdc PEMFCs which is modeled in this paper is verified with a 50 kW MATLAB/Simulink PEMFC model. The results shows that equivalent circuit models enable the designers to connect the FCs in several configurations for system level analysis.

In this work it is considered that H_2 storage requirement for bunkering at one location for a vessel is met.

A. Load sharing with ideal conditions

It is assumed that the FC performs in its maximum efficiency region which is almost from 1/3 rated power to 2/3 rated power [17]. Fig. 9 shows the load sharing while FC is designed for average power 30 kW. So, the remaining positive or negative required load power becomes the reference current input for the battery, and, during low load demand, FCs can charge the batteries also.

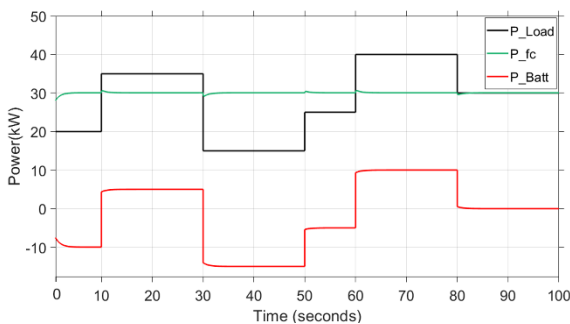


Fig. 9. The results of load sharing with FC designed for average power 30kW and battery in peak shaving mode.

In Fig. 10, it is observed that the dc bus voltage is remained constant at 1kV despite the variation in load profile. The reason is that the local controller for FC's dc-dc converter is designed in a way to regulate the dc bus voltage and the central load sharing strategy be sure that the transient power is supplied by the battery. The 50 kW, 625Vdc FC voltage also is almost stayed in its nominal operating range.

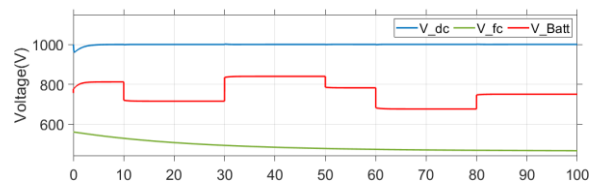


Fig. 10. The results of volage variations with FC designed for average power 30kW and battery in peak shaving mode.

During the second scenario FC is used for range extender for supplying power between 20-40 kW. This leaves a safety margin for the 50kW stack, for 10% degradation over the lifetime. Fig. 11 shows the load sharing while FC is designed for range extender and battery is dimensioned for transient power requirements. After 10 sec load is increasing 15kW from 20kW to 35kW which is in the range that FC is designed to supply the power, while due to the FC slow power slope, the battery needs to supply the transient power. It can also be seen that FC can respond faster to the sudden changes to the decrease in load power than sudden increased changes in the load power.

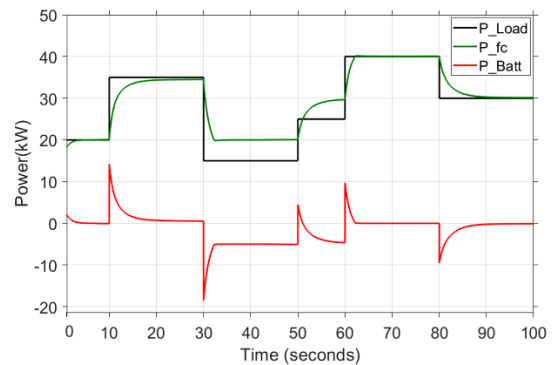


Fig. 11. The results of load sharing with FC designed for range extender 20-40kW and battery in peak shaving mode.

Fig.12 shows that the dc bus voltage is remained constant at 1kV. With comparison to the Fig. 11, there is more dc bus voltage fluctuations in acceptable level which is due to the changes in FC power which results in changes in FC current set point in the local controller.

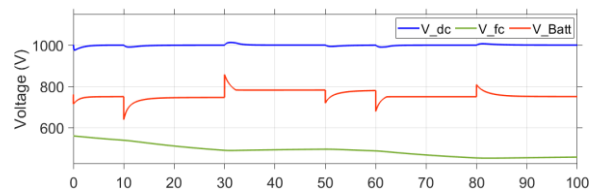


Fig. 12. The results of volage variations with FC designed for range extender 20-40kW and battery in peak shaving mode.

B. Load sharing with hydrogen flow effect

For considering the effects of the hydrogen flow rate in the modeling some assumptions for 50 kW PEMFC are considered: nominal H_2 utilization: 99.95%, hydrogen supply pressure: 1.5 bar, air supply pressure: 1 bar, and PEMFC temperature: 338 Kelvin.

In Fig. 13, the changes of the fuel flow rate is shown based on the step changes in FC current applying on 50 kW MATLAB/Simulink PEMFC model. According to the assumption considered in the modeling, the nominal fuel flow rate at nominal H_2 utilization and considering that reactants

pressure remain constant during operation is 417 lpm and the maximum fuel flow rate is 1460 lpm, which is equal to 6.95lit/sec at nominal and 24.33Lit/sec at its maximum value. The fuel flow rate is a function of FC current and increasing current requires more hydrogen be consumed. To model the effects of fuel flow rate on the FC voltage to represent it as a passive component in FC electrical equivalent circuit the changes in FC voltage is analyzed, which is shown in Fig. 14. By changes in fuel flow rate the terminal FC voltage experiences voltage drop which is modeled as a resistor $R_{H_2}(i_{fc})$ in this work.

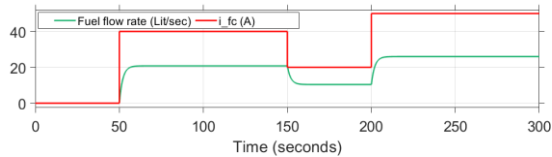


Fig. 13. The results of fuel flow rate changes based on FC step current changes.

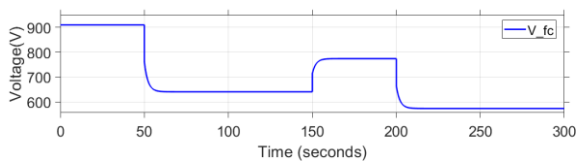


Fig. 14. The results of FC voltage changes based fuel flow changes.

Fig. 15 and Fig.16 show the FC terminal voltage for both load sharing strategies with considering the voltage drop related to the changes of hydrogen flow rate on FC's terminal voltage. When the FC is supplying the averaged power, the voltage drop related to hydrogen flow rate slightly changes based on fuel flow rate changes while when FC is designed for range extender the voltage drop due to changes in fuel flow is experiencing more transient behavior as is shown in Fig.16.

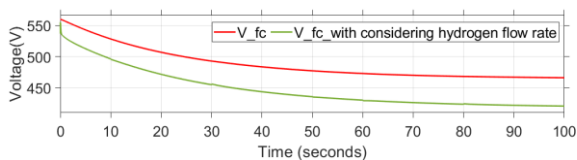


Fig. 15. The results of FC voltage change when FC is designed for average power.

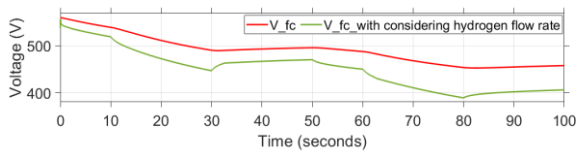


Fig. 16. The results of FC voltage change when FC is designed range extender.

V. CONCLUSIONS

In this study, the dynamic modeling and simulation of a hybrid power system for electric propulsion is presented where PEMFC in combination of battery is supplying the propulsion load. The model of the power sources with the power converters and controllers is developed as an integrated active circuit model. Power electronics converters are modeled with averaged modeling approach. The effect of the fuel flow is also added to the integrated circuit model. The active circuit model provides a simple, computationally efficient, and modular/scalable simulation model while

keeping a sufficient level of accuracy. In this approach, any electrochemical process can be modeled as an equivalent circuit block and can be integrated into the entire system model.

Time-domain simulations are presented to validate the dynamic model in presence of dynamic load. The case studies are composed of load sharing with and without the fuel flow effect. The fuel flow rate or fuel intake is logically a proportional function of output current. However, in practice, a delay is introduced due to the dynamics of the governor system. In this paper, this effect is modeled with a low-pass filter and the total fuel flow effect is modeled as a variable resistance. Equally, it could be also modeled with a dependent voltage source. When the fuel flow rate is not changing appropriate to the output current, the influence is a voltage drop on the terminal of the FC stack.

REFERENCES

- [1] Reducing greenhouse gas emissions from ships, Accessed on: March 30, 2021. [Online].
- [2] "IGF Code (2017). International Code of Safety for Ships Using Gases or other Low-Flashpoint Fuels (IGF Code). Part A.
- [3] SA Sherif, DY Goswami, EKL Stefanakos, A Steinfeld, "Handbook of hydrogen energy," 2014.
- [4] "Path to hydrogen competitiveness A cost perspective." 2020.
- [5] L. van Biert, M. Godjevac, K. Visser, and P. V. Aravind, "A review of fuel cell systems for maritime applications," *Journal of Power Sources*, vol. 327, pp. 345–364, Sep. 2016.
- [6] J. Wang, "System integration, durability and reliability of fuel cells: Challenges and solutions," *Applied Energy*, vol. 189, pp. 460–479, Mar. 2017.
- [7] P. Ghimire, D. Park, M. K. Zadeh, J. Thorstensen, and E. Pedersen, "Shipboard Electric Power Conversion: System Architecture, Applications, Control, and Challenges [Technology Leaders]," *IEEE Electrification Magazine*, vol. 7, no. 4, pp. 6–20, Dec. 2019.
- [8] J. T. Pukrushpan, H. Peng, and A. G. Stefanopoulou, "Control-Oriented Modeling and Analysis for Automotive Fuel Cell Systems," *Journal of Dynamic Systems, Measurement, and Control*, vol. 126, no. 1, pp. 14–25, Apr. 2004.
- [9] D. Torregrossa, M. Bahramipanah, E. Namor, R. Cherkaoui, and M. Paolone, "Improvement of Dynamic Modeling of Supercapacitor by Residual Charge Effect Estimation," *IEEE Transactions on Industrial Electronics*, vol. 61, no. 3, pp. 1345–1354, Mar. 2014.
- [10] J. Larminie and A. Dicks, "Fuel Cell Systems Explained," 2nd ed. Wiley, 2003.
- [11] N. Shakeri, M. Zadeh, and J. Bremnes Nielsen, "Hydrogen Fuel Cells for Ship Electric Propulsion: Moving Toward Greener Ships," *IEEE Electrification Mag.*, vol. 8, no. 2, pp. 27–43, Jun. 2020.
- [12] A. Haxhiu, J. Kyyrä, R. Chan, and S. Kanerva, "Improved Variable DC Approach to Minimize Drivetrain Losses in Fuel Cell Marine Power Systems," *IEEE Transactions on Industry Applications*, vol. 57, no. 1, pp. 882–893, Jan. 2021.
- [13] C. Raga et al., "Black-Box Model, Identification Technique and Frequency Analysis for PEM Fuel Cell With Overshooting Transient Response," *IEEE Transactions on Power Electronics*, vol. 29, no. 10, pp. 5334–5346, Oct. 2014.
- [14] M. K. Zadeh, L.-M. Saublet, R. Gavagsaz-Ghoachani, B. Nahid-Mobarakeh, S. Pierfederici, and M. Molinas, "Energy management and stabilization of a hybrid DC microgrid for transportation applications," in *2016 IEEE Applied Power Electronics Conference and Exposition (APEC)*, Mar. 2016, pp. 3397–3402.
- [15] D. Park and M. Zadeh, "Modeling and Predictive Control of Shipboard Hybrid DC Power Systems," *IEEE Transactions on Transportation Electrification*, vol. 7, no. 2, pp. 892–904, Jun. 2021.
- [16] D. Park, M. K. Zadeh, and R. Skjetnet, "DC-DC Converter Control for Peak-Shaving in Shipboard DC Power System via Hybrid Control," in *2020 15th IEEE Conference on Industrial Electronics and Applications (ICIEA)*, Nov. 2020, pp. 681–686.
- [17] P. Thounthong, S. Raël, and B. Davat, "Energy management of fuel cell/battery/supercapacitor hybrid power source for vehicle applications," *Journal of Power Sources*, vol. 193, no. 1, pp. 376–385, Aug. 2009.